Epilepsy dynamics of an astrocyte-neuron model with ammonia intoxication

Zhixuan Yuan(袁治轩)[1], Mengmeng Du(独盟盟)[2], Yangyang Yu(于羊羊)[1], and Ying Wu(吴莹)[1,†]

[1] *State Key Laboratory for Strength and Vibration of Mechanical Structures, Shaanxi Engineering Laboratory for Vibration Control of Aerospace Structures, School of Aerospace Engineering, Xi'an Jiaotong University, Xi'an* 710049, *China*

[2] *School of Mathematics and Data Science, Shaanxi University of Science and Technology, Xi'an* 710000, *China*

(Received 5 February 2022; revised manuscript received 10 April 2022; accepted manuscript online 7 May 2022)

Experimental records in the cerebral cortex indicate that ammonia injection can lead to seizures. Considering that astrocytes play a vital role in mediating the uptake and absorption of ammonium ions in the extracellular space of the cortical circuit, we constructed a new astrocyte neuron coupling model, which is composed of a neuron and its astrocytes connected through the extracellular space, taking into account of the influence of extracellular ammonium ions. The numerical results verified the previous experimental observation that obtained epileptic firing modes of neurons and postsynaptic GABA reversal potential depolarization triggered by ammonia injection. In addition, we also determined the concentration–response relationship between the ammonium ion concentration and the time of entering epilepsy and predicted the threshold of the ammonium ion concentration for the onset of epilepsy.

Keywords: ammonia, neuron, astrocyte, epilepsy

PACS: 05.45.–a, 64.70.qj, 87.19.L–, 87.19.lk **DOI:** 10.1088/1674-1056/ac6dbc

1. Introduction

Ammonia is a common protein metabolic waste that can accumulate in many metabolic disorders and contribute to neurological dysfunction, including cognitive impairment, seizures, stupor and even death.[1,2] In addition, ammonia homeostasis is vital in the brain because ammonium ions promote the release of the excitotoxic neurotransmitter glutamate during neuronal discharge.[3] In the brain, glutamine synthetase, an enzyme that removes ammonia and glutamate, has a higher affinity for ammonia than for glutamate.[4,5] Astrocytes play a key role in the metabolism of ammonia and the putative neurotransmitters glutamate and γ-aminobutyric acid by forming compartments related to glutamine synthetase, the primary enzyme necessary for ammonia detoxification.[6,7] The main route by which astrocytes detoxify ammonia is to absorb excess ammonia and combine it with glutamate intracellularly through glutamine synthase to produce nontoxic glutamine.[8,9] The experimental data suggested that the K^+ uptake channel on the astrocyte membrane transports ammonium ions through the membrane at high ammonia concentrations via their occupation of the uptake channel responsible for transporting potassium ions under normal physiological conditions.[10] The K^+ uptake channel of astrocytes primarily includes the Na^+/K^+-ATPase pump and Kir4.1 channel (inward rectifier K^+ channel), which absorbs excess K^+ in the extracellular environment. Many experimental studies have shown that the Kir4.1 channel plays an important role in the local absorption of extracellular K^+.[11–13] For example, astrocyte Kir4.1 channel deficits lead to neuronal dysfunction in Huntington's disease model mice.[14] Therefore, we investigated the dynamic mechanism of extracellular K^+ concentration change and pathological epileptic discharge caused by K^+ uptake disorder under the condition of extracellular high ammonia with a computational neuron-astrocyte model.

Research exploring the relationship between astrocyte K^+ uptake channel regulation of K^+ and seizures through theoretical analysis has emerged in recent years.[15–20] Cressman *et al.* combined active and passive local K^+ uptake via astrocytes into a simplified K^+ uptake function in the shape of a sigmoid that depends only on the extracellular K^+ concentration.[15,16] Østby *et al.* studied the mechanisms of extracellular space contraction and potassium clearance during neuronal discharge by constructing a volume dynamic model[21,22] for astrocyte cotransporters (e.g., $Na^+/K^+/2Cl^-$ and K^+/Cl^-) and Na^+/K^+-ATPase pumps. Witthof *et al.* and Sibille *et al.* mathematically modelled the Kir4.1 channel, which depends on both the astrocytic membrane potential and extracellular K^+ concentration, respectively,[23,24] and they verified the prominent role of Kir4.1 channels in regulating excess $[K^+]_o$. Du *et al.* constructed an astrocyte-neuron network module consisting of a neuron and four surrounding connected astrocytes and validated that both Kir4.1 channels and gap junctions play an important role in regulating the $[K^+]_o$ concentration.[25]

Considering these findings, we built a model of an astrocyte-neuron model, considering the Kir4.1 channel, $Na^+/K^+/Cl^-$, K^+/Cl^- cotransporters and Na^+/K^+-ATPase

†Corresponding author. E-mail: wying36@xjtu.edu.cn

© 2023 Chinese Physical Society and IOP Publishing Ltd

pumps. In order to describe the effect of ammonium ions on extracellular potassium ion concentration, we created an h function based on experimental data fitting to revise the Kir4.1 channel model.[10,26] Based on the model, we reproduced the process of neuronal epileptic discharge caused by injection of ammonium chloride found in physiological experiments,[10,26] and the mechanism of neuronal E_{GABA} depolarization caused by impaired potassium buffer of astrocytes in ammonia neurotoxicity was also obtained. In addition, the timing of neurons entering epilepsy decreased with increasing ammonium ion concentrations, and the ammonium ion concentration threshold causing epilepsy was determined.

2. Materials and methods

To validate the intoxication effect of ammonium ions on neuronal electric activities, we constructed a model consisting of three parts: a neuron, an astrocyte and the connected extracellular space (Fig. 1). In Fig. 1, several critical factors regulating the extracellular K^+ concentration are apparent:[11,12,15,17] K^+ current passing through the neuronal membrane, cotransporters NKCC and KCC, Na^+/K^+-ATPase pumps of the neuron and the astrocyte, Kir4.1 channels in astrocytes, and spatial diffusion of K^+ in the extracellular space. However, in the situation of ammonia injection, the Kir4.1 channel, which transports K^+ under normal physiological conditions, cannot transport K^+ but NH_4^+ (see Fig. 1).

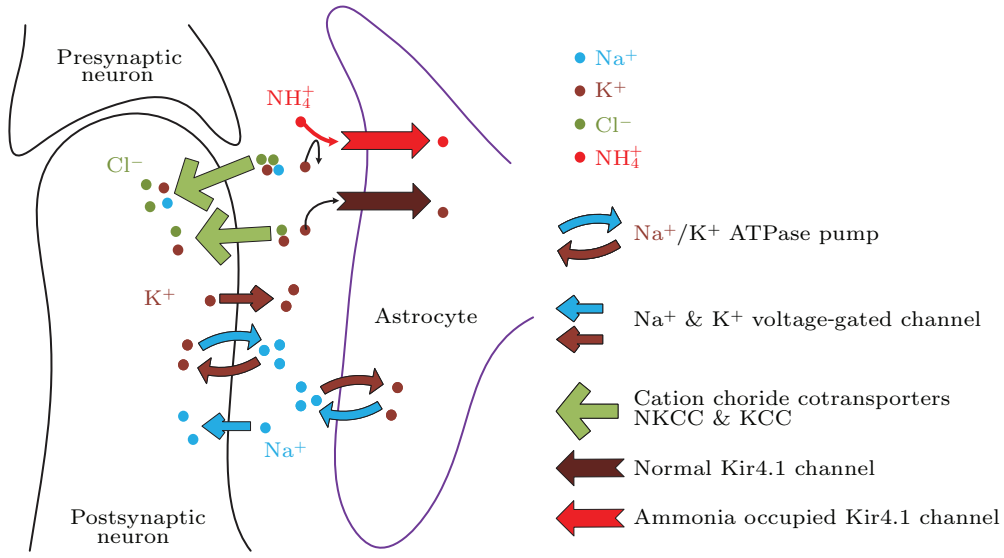


Fig. 1. The diagram of this tri-compartment model includes the neuron, the extracellular space and the astrocyte, taking into account of the influence of ammonium ions. NKCC: $Na^+/K^+/Cl^-$ cotransporter, the transportation ratio is $1Na^+ : 1K^+ : 2Cl^-$; KCC: K^+/Cl^- cotransporter, the transportation ratio is $1K^+ : 1Cl^-$; the Kir4.1 channel (inward rectifier potassium ion channel) transports potassium ions under normal physiological conditions, ammonium ions will occupy the position of potassium ions and be transported by the Kir4.1 channel in the case of ammonia neurotoxicity.

2.1. Neuron model

We used the modified Hodgkin–Huxley model containing sodium, potassium and chloride ion currents[25]

$$\begin{aligned} C_{\rm m}\frac{{\rm d}V}{{\rm d}t} &= I_{\rm Na}+I_{\rm K}+I_{\rm Cl},\\ I_{\rm Na} &= -g_{\rm Na}m^3h(V-V_{\rm Na})-g_{\rm NaL}(V-V_{\rm NaL}),\\ I_{\rm K} &= -\left(g_{\rm K}n^4+\frac{g_{\rm AHP}[{\rm Ca}]_{\rm N}}{1+[{\rm Ca}]_{\rm N}}\right)(V-V_{\rm K})\\ &\quad -g_{\rm KL}(V-V_{\rm KL}),\\ I_{\rm Cl} &= -g_{\rm Cl}(V-V_{\rm Cl}), \end{aligned} \tag{1}$$

where $g_{\rm Na}$, $g_{\rm NaL}$, $g_{\rm K}$, $g_{\rm KL}$ and $g_{\rm Cl}$ denote the conductances corresponding to the Na^+, Na^+ leak, K^+, K^+ leak and Cl^- currents, respectively. Correspondingly, V_s represents the reversal potential of the s channel ($s = Na^+$, K^+, Cl^-, Na^+ leak, K^+ leak).

$$\frac{{\rm d}s}{{\rm d}t}=\alpha_s(1-s)-\beta_s s, \quad s=m,n,h. \tag{2}$$

The after-hyperpolarization current $I_{\rm AHP}=\frac{g_{\rm AHP}[{\rm Ca}]_{\rm N}}{1+[{\rm Ca}]_{\rm N}}(V-V_{\rm K})$ is integrated into $I_{\rm K}$, in addition to the activation and inactivation sodium ion (Na+) gate m^3 and h as well as the potassium channel opening probability n^4.

The coefficients in Eq. (2) are given by

$$\begin{aligned} \alpha_m &= 0.1\frac{V+30}{1-\exp[-0.1(V+30)]},\\ \beta_m &= 4\exp\left[\frac{-(V+55)}{18}\right],\\ \alpha_n &= 0.01\frac{V+34}{1-\exp[-0.1(V+34)]},\\ \beta_n &= 0.125\exp\left[\frac{-(V+44)}{80}\right],\\ \alpha_h &= 0.07\exp\left[\frac{-(V+44)}{20}\right],\\ \beta_h &= \frac{1}{1+\exp[-0.1(V+14)]}. \end{aligned} \tag{3}$$

$[Ca]_N$ corresponds to the intracellular calcium concentration, and the dynamic equation is

$$\frac{d[Ca^{2+}]_N}{dt} = -0.002 g_{Ca}(V_N - V_{Ca})/1 + \exp(-(V_N+25)/2.5) - [Ca]_N/80. \quad (4)$$

The reversal potentials of Na^+ K^+ and Cl^- are given by the Nernst equation

$$V_{Na} = 26.64 \ln\left(\frac{[Na^+]_o}{[Na^+]_N}\right),$$
$$V_K = 26.64 \ln\left(\frac{[K^+]_o}{[K^+]_N}\right),$$
$$V_{Cl} = 26.64 \ln\left(\frac{[Cl^-]_N}{[Cl^-]_o}\right). \quad (5)$$

2.2. Balance of ion fluxes

The K^+ value is constantly updated by the K^+ current across the neuronal membrane, Na^+/K^+-ATPase pumps, KCC (K^+/Cl^-), NKCC ($Na^+/K^+/2Cl^-$) cotransporters of the neuron, K^+ spatial diffusion, Na^+/K^+-ATPase pumps of the astrocyte and the Kir4.1 channel.[17,24] The current passing through the cell membrane will cause a change in the ion concentration inside and outside the cell. The current I passing through the membrane is equal to the ion flow J per unit time. Therefore, the dynamics of the K^+ concentration in neurons and astrocytes and the extracellular space are as follows:

$$\begin{aligned}
\frac{d[K^+]_o}{dt} &= J_{I_K} - 2J_{pump,N} - 2J_{pump,A} + J_{Kir} - J_{diff} - J_{KCC} - J_{NKCC},\\
\frac{d[K^+]_N}{dt} &= (-J_{I_K} + 2J_{pump,N} + J_{KCC} + J_{NKCC}) v_{rate1},\\
\frac{d[K^+]_A}{dt} &= (-J_{Kir} + 2J_{pump,A} - k_A([K^+]_A - [K^+]_{AE})) v_{rate2}, \quad (6)
\end{aligned}$$

Similar to the K^+ dynamics, the Na^+ value is continuously updated by the Na^+ current crossing through the neuronal membrane, Na^+/K^+-ATPase pumps, NKCC ($Na^+/K^+/2Cl^-$) cotransporter of the neuron, and Na^+/K^+-ATPase pumps of the astrocyte.[17,24] The Na^+/K^+-ATPase pump exchanges two K^+ for three Na^+ ions. Thus, the dynamics of the Na^+ concentration in neurons and astrocytes and the extracellular space are as follows:

$$\begin{aligned}
\frac{d[Na^+]_o}{dt} &= J_{I_{Na}} + 3J_{pump,N} + 3J_{pump,A} - J_{KCC} - J_{NKCC},\\
\frac{d[Na^+]_N}{dt} &= (-J_{I_{Na}} - 3J_{pump,N} + J_{KCC} + J_{NKCC}) v_{rate1},\\
\frac{d[Na^+]_A}{dt} &= (-3J_{pump,A} + J_{NaL,A}) v_{rate2}. \quad (7)
\end{aligned}$$

In the same way, Cl^- is changed by the Cl^- current, KCC (K^+/Cl^-) and NKCC ($Na^+/K^+/2Cl^-$) cotransporters of the neuron, while the chloride ion in astrocytes has not been considered

$$\begin{aligned}
\frac{d[Cl^-]_o}{dt} &= J_{I_{Cl}} - J_{KCC} - 2J_{NKCC},\\
\frac{d[Cl^-]_N}{dt} &= (-J_{I_{Cl}} + J_{KCC} + 2J_{NKCC}) v_{rate1}. \quad (8)
\end{aligned}$$

In addition, the terms in Eqs. (6)–(8) are given as follows:

$$\begin{aligned}
J_{pump,N} &= \rho\left(\frac{1}{1+\exp(25-[Na^+]_N)/3)}\right) \times \left(\frac{1}{1+\exp(8-[K^+]_o)}\right),\\
J_{pump,A} &= \frac{1}{3}\rho\left(\frac{1}{1+\exp(25-[Na^+]_A)/3)}\right) \times \left(\frac{1}{1+\exp(8-[K^+]_o)}\right),\\
J_{diff} &= \varepsilon([K^+]_o - K_{bath}),\\
J_{KCC} &= U_{KCC} \ln\left(\frac{[K^+]_N[Cl^-]_N}{[K^+]_o[Cl^-]_o}\right),\\
J_{NKCC} &= U_{NKCC} f([K^+]_o) \ln\left(\frac{[Na^+]_N[K^+]_N([Cl^-]_N)^2}{[Na^+]_o[K^+]_o([Cl^-]_o)^2}\right),\\
f([K^+]_o) &= \frac{1}{1+\exp(16-[K^+]_o)}, \quad (9)
\end{aligned}$$

where ρ, U_{KCC} and U_{NKCC} are the strengths of the Na^+/K^+-ATPase pump, KCC cotransporters and NKCC cotransporters, respectively. ε and K_{bath} represent the potassium diffusion coefficient and bath potassium concentration, respectively.

2.3. Astrocyte model

The astrocyte membrane potential V_A is described as follows:[25]

$$C_A \frac{V_A}{dt} = -I_{Kir} - I_{lA}, \quad (10)$$

where C_A is the astrocytic capacitance and I_{Kir} and I_{lA} are the inward rectifier Kir4.1 channel and leak current, respectively, and they are given by

$$\begin{aligned}
I_{Kir} &= g_{Kir} h([NH_4^+]_o) \sqrt{[K^+]_o}(V_A - V_{Kir}),\\
V_{Kir} &= E_{Kir} \ln\left(\frac{[K^+]_N}{[K^+]_A}\right),\\
I_{lA} &= g_{lA}(V_A - V_{lA}), \quad (11)
\end{aligned}$$

where g_{Kir} and E_{Kir} are the conductance and the Nernst constant for the astrocyte Kir4.1 channels, respectively. Experimental results[10] show that the increase of $[NH^{4+}]_o$ leads to the increase of $[K^+]_o$ in the extracellular environment of the astrocyte. Physiologically, $[NH^{4+}]_o$ occupy the position of $[K^+]_o$ on the Kir channel. All Kir channels on the astrocyte membrane are occupied with the continuous increase of $[NH^{4+}]_o$, and the extracellular K^+ also reaches the maximum.

To account for the change of $[NH^{4+}]_o$ concentration in Kir4.1 channel on the astrocyte membrane, we created the function $h([NH_4^+]_o)$ according to its biophysical properties[10]

$$h([NH_4^+]_o) = \frac{1}{1+\exp(4(2.5-[NH_4^+]_o))}, \quad (12)$$

where the parameters were obtained by means of data fitting with the experimental results.[10,26]

The values of the parameters used in the model are listed in Table 1. In the simulation, we used the Runge–Kutta algorithm with a step size of 0.01 ms.

Table 1. Parameters and constants in the simulation.

Parameter	Value and units	Description
C_m	1 μF/cm^2	Membrane capacitance of neuron
g_{Na}	100.0 mS/cm^2	Conductance of the sodium current
g_{NaL}	mS/cm^2	Conductance of the sodium leak current
g_K	40.0 mS/cm^2	Conductance of the potassium current
g_{AHP}	0.01 mS/cm^2	Conductance of the after-hyperpolarization current
g_{KL}	0.05 mS/cm^2	Conductance of the potassium leak current
g_{Cl}	0.05 mS/cm^2	Conductance of the chloride current
g_{Ca}	0.1 mS/cm^2	Conductance of the calcium current
V_{Ca}	120 mV	Reversal potential of the calcium current
v_{rate1}	7.0	The volume ratio of the neuron to extracellular space
v_{rate2}	3.0	The volume ratio of the astrocyte to extracellular space
k_A	0.05	The rate at which the astrocyte K_+ concentration decays to its baseline state
$[K^+]_{AE}$	100	The resting state equilibrium K_+ concentration
ρ	1.25 mM/s	Na^+/K^+-ATPase pump strength
ε	1.2 mM/s	Potassium diffusion rate
U_{KCC}	0.3 mM/s	Maximal KCC cotransporter strength
U_{NKCC}	0.1 mM/s	Maximal NKCC cotransporter strength
C_A	75 pF	Membrane capacitance of astrocyte
g_{lA}	0.17 m/(M·ms)	Astrocytic leak conductance
V_{lA}	70 mV	Astrocytic leak current reversal potential

3. Results

3.1. Epilepsy caused by ammonia neurotoxicity

The experiment record of changes in ammonium ion concentration from Fig. 2d in Ref. [10] is shown in Fig. 2(a). The red part indicates the time of ammonium chloride solution injection, and the yellow part indicates the occurrence of epilepsy *in vivo* in the mouse brain. Although the concentration of the injected solution is constant, the concentration of ammonium ions will not be constant when it reaches the region outside neurons and astrocytes. Correspondingly, we simulate the changing concentration of ammonium ions as an external input, which is plotted in Fig. 2(b).

After the input of ammonium ions was determined, we started the simulation to capture the results that the input lasted for 15 minutes. The neuronal membrane potential (V_N) and extracellular potassium ion ($[K^+]_o$) results are shown in Figs. 2(c) and 2(d), respectively. The discharge pattern of the neuron changes from periodic cluster discharge at the beginning (area 1) to the epileptic state (area 2) at approximately 360 s (6 min) and is sustained in the epileptic discharge mode (area 3). Consistent with the changes in neuronal discharge patterns, the concentration of potassium ions remains at a low level at first (area 1), then gradually increases by more than 20 mM (area 2), and finally maintains a high level (area 3). The three marked areas in Figs. 2(c) and 2(d) are magnified in Figs. 2(e)–2(g), as well as the $[NH_4^+]$ and astrocytic $[K^+]_o$ are shown in Figs. 2(e)–2(g) for more detailed visualisation.

The concentration of ammonium ions gradually increases with the injection of ammonium chloride solution (Figs. 2(e)–2(g)), and the excess ions occupy the astrocytic Kir4.1 channel that originally transported potassium ions. Consequently, the concentration of $[K^+]_o$ increases until 20 mM (see right half of Fig. 2(f)), causing the neuron to become epileptic shown in the time history diagram of V_N in Fig. 2(f). This type of spontaneous epileptic seizure has been observed in various experimental recordings.[27–29] In addition, the concentration of potassium ions in astrocytes decreases due to the lack of potassium ion absorption, which is also a manifestation of astrocyte potassium buffer failure in ammonia neurotoxicity. Epileptic states are also marked red in the simulation results (Fig. 2(h)) for direct comparison with the experimental result (Fig. 2(a)). On the whole, the neuron remains in a periodic cluster discharge pattern when the ammonium ion is still low (almost less than 270 s), accompanying a lower amplitude of oscillating $[K^+]_o$. The epileptic neuron is sustained at a higher NH_4^+ (almost more than 380 s), causing an increase in $[K^+]_o$ that reaches a peak value of 20 mM.

The numerical simulation results are consistent with the experimental record, and the rationality of the model is verified.

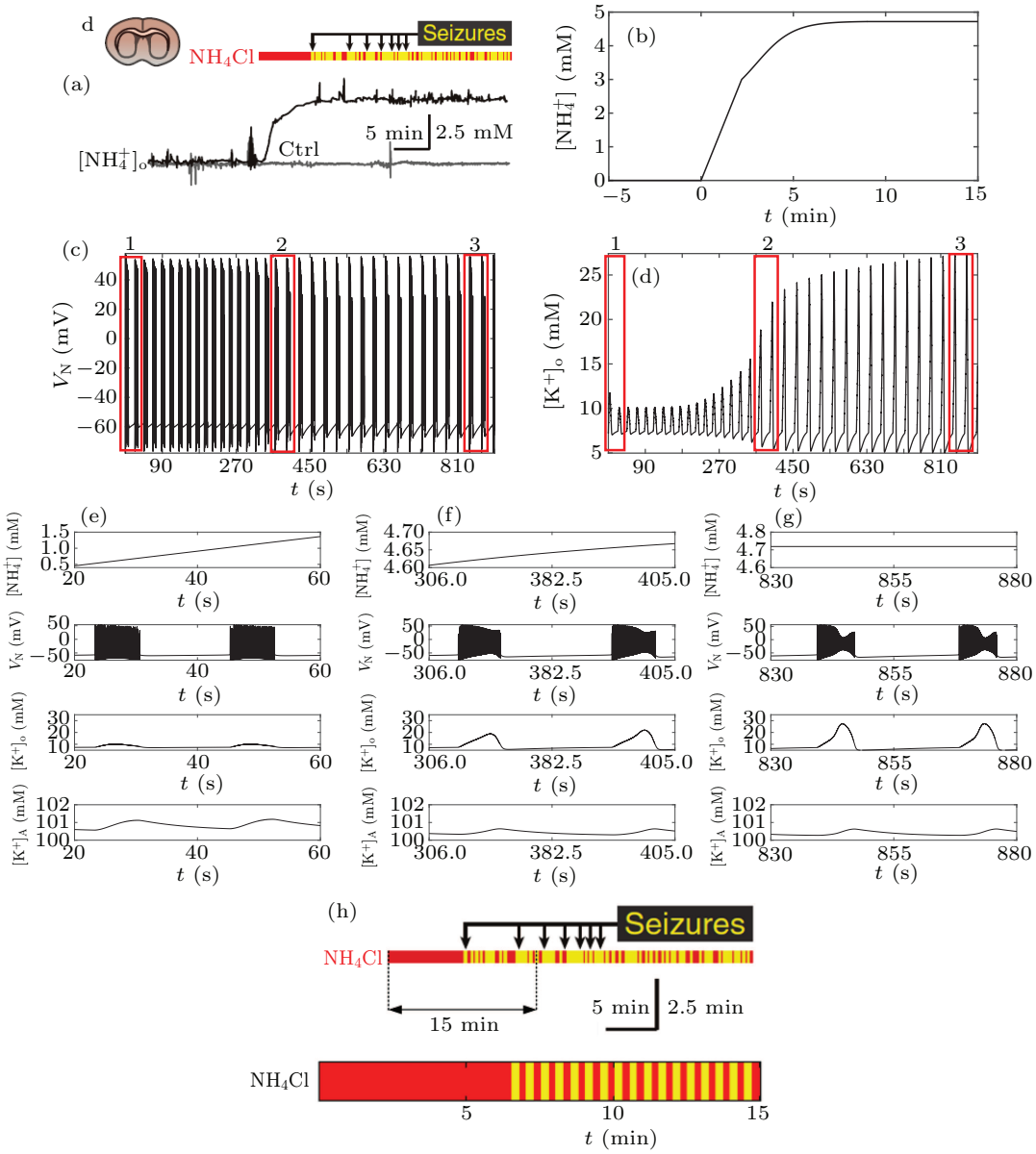


Fig. 2. (a), (b) The experimental record in Ref. [10] Fig. 2d and corresponding simulated input in this section. (c), (d) Time histories of neuronal membrane potential (V_N) and extracellular potassium ions ($[K^+]_o$) under the condition of simulated varying ammonium ion concentrations (b). (e)–(g) The first, middle and last two clusters of the firing patterns shown in (c) and the corresponding ammonium ion concentration ($[NH_4^+]_o$), extracellular potassium ion concentration ($[K^+]_o$), astrocytic membrane potential (V_A) and astrocyte intracellular potassium ion concentration ($[K^+]_A$). (h) Experimental recording (top) and simulation (bottom) of the neuronal modes under ammonium chloride injection, and yellow parts represent the neurons in the epileptic state.

3.2. Neuronal E_{GABA} depolarization caused by ammonia neurotoxicity

The inhibitory effects of γ-aminobutyric acid (GABA) are mainly mediated by two different types of postsynaptic receptors: $GABA_A$ and $GABA_B$.[30] Simulation of hippocampal pyramidal cells leads to transient glutamatergic excitation, followed by rapid inhibitory postsynaptic potential (IPSP) induced by chloride influx through $GABA_A$ receptor gated ion channels,[31,32] therefore, the chloride ion reversal potential can be taken place of the GABA reversal potential.

In this part, the chloride ion reversal potential (E_{Cl}, namely V_{Cl} in Eq. (5)) was substituted to obtain the change in postsynaptic GABA reversal potential (E_{GABA}) caused by ammonia neurotoxicity and the input of ammonium ions was set to a constant value. The responses of the neuron-astrocyte coupling system at null (0 mM) and high (4.8 mM) levels of ammonium ion were first tested (Fig. 3).

These results can be predicted because they are similar to the two input forms in the previous part. However, the constant and variable inputs are indeed different. Cluster-periodic firing of the neuron occurs at the lower level ($[NH_4^+]_o = 0$ mM), while the neuron is in an epileptic state at the higher level ($[NH_4^+]_o = 4.8$ mM). The amplitude of extracellular K^+ oscillation increases consistent with the change in neuronal discharges, along with the decrease in K^+ concentration in astrocytes. In addition, two clusters of neuronal electric activities in each case and the reversal potentials of Na^+, K^+ and Cl^- were selected for clearer observation (Fig. 4).

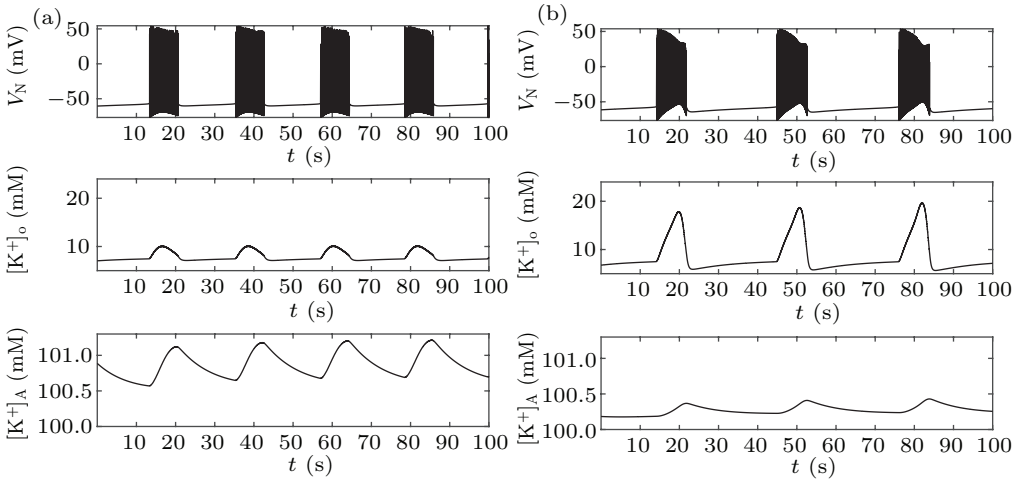


Fig. 3. Time histories of neuronal membrane potential (V_N), extracellular potassium ion ($[K^+]_o$) and astrocyte intracellular potassium ion ($[K^+]_A$) at (a) low ($[NH_4^+]_o = 0$ mM) or (b) high ($[NH_4^+]_o = 4.8$ mM) levels of constant ammonium ion.

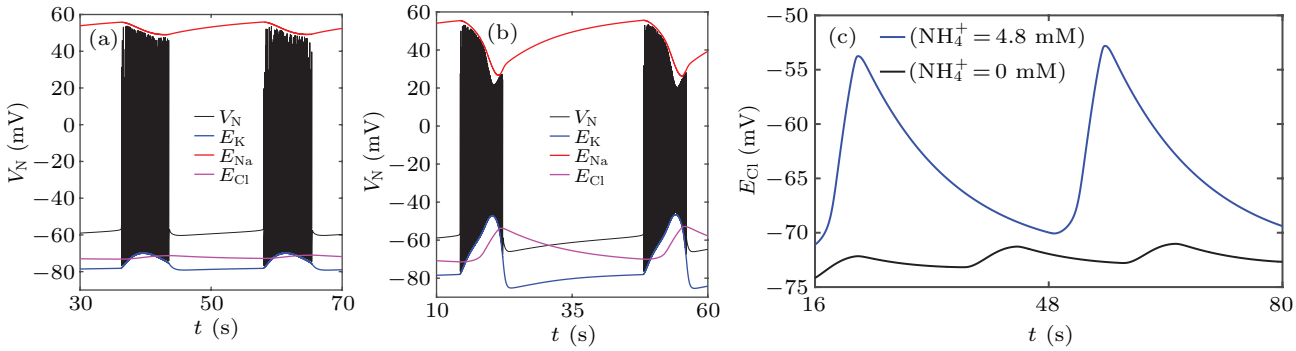


Fig. 4. (a) and (b) Time histories of neuronal membrane potential (V_N), reversal potentials of Na^+ (E_{Na}), K^+ (E_K) and Cl^- (E_{Cl}) at low ($[NH_4^+]_o = 0$ mM) or high ($[NH_4^+]_o = 4.8$ mM) levels of ammonium ion. (c) Chloride reversal potential (E_{Cl}) under each case of the different ammonium ion concentrations in the simulation.

Figure 4 shows the neuronal membrane potential and three kinds of ion reversal potentials under two ammonium ion concentrations. The reversal potential of chloride ions (E_{Cl}) in ammonia neurotoxicity (Fig. 4(b)) is clearly higher than that in the absence of ammonia (Fig. 4(a)), which is consistent with the experimental recording (Fig. 3j in Ref. [10]). In addition, E_{Cl} in the two cases are plotted in Fig. 4(c) for a more visual comparison. This phenomenon reflects the depolarization of the postsynaptic GABA potential (E_{GABA}) caused by the increase in ammonium ion concentration and observed both in experiments and simulations.

In addition, the effects of ammonium ions on E_{GABA} were also observed in other experimental records (Fig. 5(a) from Fig. 2A in Ref. [26]). With the increase in NH_4^+, the ratio of E_{GABA} to itself at $[NH_4^+]_o = 0$ mM increases and gradually stabilizes under higher ammonia concentrations. Additionally, the new model was applied for the simulation, and the result is shown in Fig. 5(b). The numerical results show that the ratios have same pattern as the experimental recording, and the values of ratios for lower and higher levels of ammonia ion concentration are similar to the experimental results. However, when the ammonium ion changes only by 0.1 mM from 0.4 mM to 0.5 mM, the ratio increases from 1 to the maximum, demonstrating a faster rate than that in the experiment.

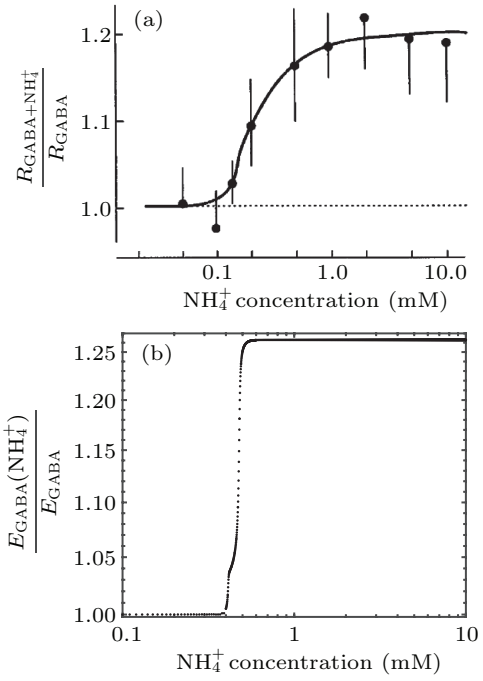


Fig. 5. Comparison of the ratio of GABA reversal potential (E_{GABA}, namely R_{GABA}) to it at $[NH_4^+]_o = 0$ mM under different ammonium ion concentrations in the experiment (Fig. 2A in Ref. [26]) and the simulation result.

Thus, the results in Subsections 3.1 and 3.2 show that ammonia intoxication in the nervous system induces neuronal epileptic firing modes and depolarization of E_{GABA}, which are consistent with the corresponding experimental evidence. The model constructed in this paper can consequently reflect the nervous system response to ammonia neurotoxicity to some extent.

3.3. Effects of ammonium ion concentration on neuronal electrical activity

The first part takes the changing ammonium ion as the input, while the last part examines the response of the nervous system under conditions of high ammonia or no ammonia. Specifically, the critical ammonium ion concentration for inducing epilepsy in this system needs to be studied.

First, the electrical activity response of the coupling system was observed when the ammonium ion concentration assumed several values between 0 mM and 5 mM as the external input (Fig. 6). Only the neuronal membrane potential (V_{N}) and the extracellular potassium ion ($\mathrm{K}_{\mathrm{o}}^{+}$) are plotted for more concise visualisation.

The discharge mode of the neuron hardly changes when the NH_4^+ concentration is lower than 4 mM (Figs. 6(a) and 6(b)), it continues to retain a continuous periodic cluster firing pattern, and only the peak value of the $[\mathrm{K}^+]_{\mathrm{o}}$ concentration increases slightly. However, the firing mode changes until the NH_4^+ concentration reaches 4.5 mM. Figure 6(c) shows that the neuron exhibits spontaneous epilepsy approximately 700 s after a lasting cluster discharge. In the case of higher ammonium ion concentration ($[\mathrm{NH}_4^+] = 5$ mM), the neuron exhibits direct epileptic seizures (Fig. 6(d)).

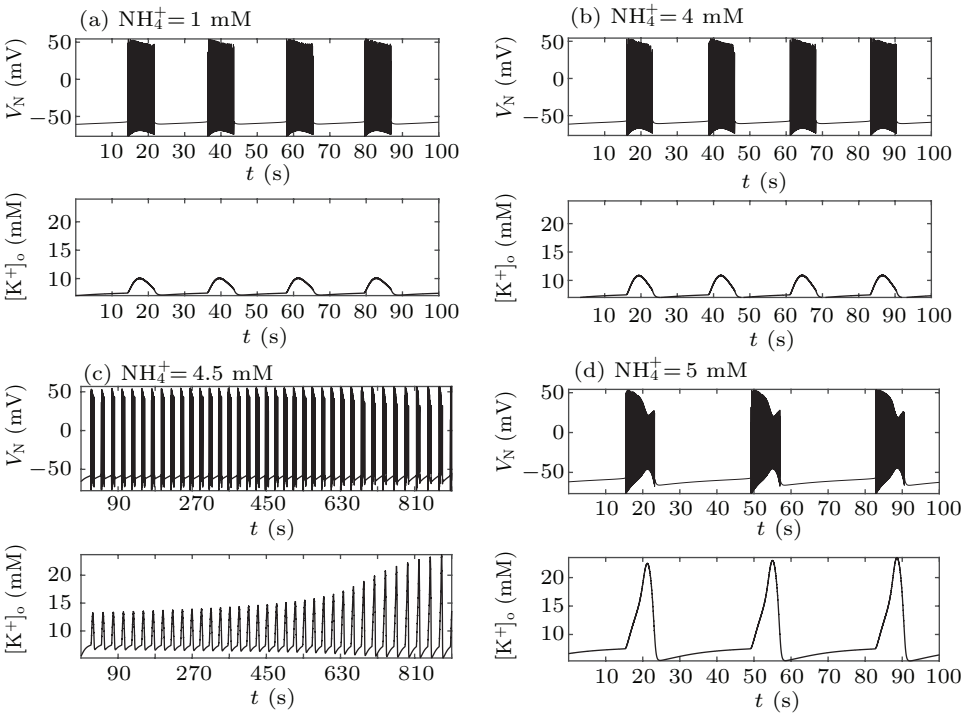


Fig. 6. Time histories of neuronal membrane potential (V_{N}) and extracellular potassium ions ($[\mathrm{K}^+]_{\mathrm{o}}$) under different ammonium ion concentrations as constant inputs.

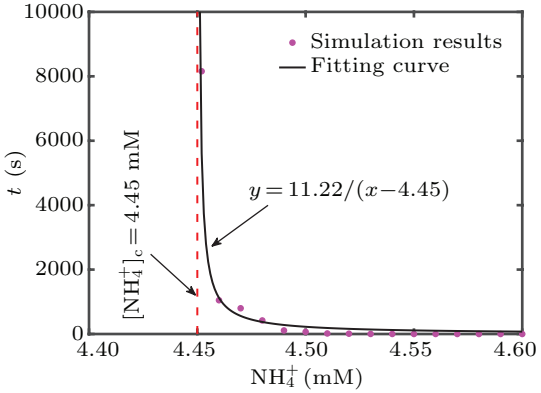


Fig. 7. The timing of entering epileptic state under different ammonium ion concentrations in the simulation results, following with the fitting curve. $[\mathrm{NH}_4^+]_{\mathrm{c}} = 4.45$ mM indicates the critical value.

Compared with the neuron directly entering the epileptic state in Fig. 6(d), the neuron in Fig. 6(c) takes much longer. In order to explore whether there is such a time extension phenomenon with the change of ammonia ion concentration, we calculate the timing of neurons entering epilepsy in ammonium ion concentration ranging from 4.4 mM to 4.6 mM (Fig. 7). As shown in Fig. 7, the moment for entering neuronal epilepsy occurs later with a decrease in the NH_4^+ concentration from 4.6 mM, which indicates there is critical slowing down. The critical value, which sufficiently induces epileptic neurons, is obtained by fitting the inverse proportional function: $[\mathrm{NH}_4^+]_{\mathrm{c}} = 4.45$ mM for the critical slowing down theory. Moreover, neurons will rapidly enter spontaneous epilep-

tic seizures with more severe toxicity.

4. Discussion and conclusion

Ammonia is toxic to the central nervous system (CNS), and elevated concentrations are a potential complicating factor leading to neurological abnormalities in several diseases, especially epilepsy.[33,34] Ammonia enters the brain from the periphery,[35] alters glial metabolism and accompanies changes in glial morphology for astrocytic detoxification.[36–39] In addition, ammonia is also a direct neurotoxicant that inhibits Na^+/K^+-ATPase pump activity[40] and inactivates Cl^- extrusion pumps.[41] To clarify how ammonium ions in the nervous system induce spontaneous epileptic discharges and affect the normal electrophysiological activities of the astrocyte-neuron system, we constructed a novel neuron-extracellular space-astrocyte coupling model via introducing the h function in shape of sigmoid in the Kir4.1 channel model contained extracellular NH_4^+.

Our model numerically verifies the previous experimental observations: neurons slowly produce epileptic discharges, and postsynaptic GABA reversal potential increases under ammonia injection. The simulation results are validated by the experimental recording.[10,26,42] In addition, we also obtained the threshold of the ammonium ion concentration for the onset of epilepsy through fitting the relationship between the concentration of NH_4^+ and the time of neuron entering epilepsy.

There are many potassium channels on the membranes of neuronal cells: K^+ current channel, Na^+/K^+-ATPase pumps, $Na^+/K^+/2Cl^-$ and K^+/Cl^- cotransporters. Astrocytic Na^+/K^+-ATPase pumps occupied by ammonium ions were attempted, but the simulation results were unsatisfactory with the experiment; thus, the Kir channel is selected in this paper. Additionally, these channels on the neuronal membrane have been assumed to be ineffective in the case of ammonia intoxication, which has no effect on the discharge activity of neurons. In addition, the spatial impact of ammonia intoxication also requires further research. At that time, multiple neurons, astrocytes and even neuron-astrocyte network structures need to be constructed, and excitatory or inhibitory connections between neurons and gap junctions will naturally be taken into account. This may lead to more real and in-depth results on a broader scale.

It is well established that ammonia neurotoxicity leads to neuronal hyperexcitability and epileptic activity. Astrocyte dysfunction and potassium buffering failure should be considered promising targets for new therapies. This study aims to deeply understand the role of ion exchange in the extracellular environment during seizures caused by the toxic action of ammonia to promote the construction of a more accurate dynamic neuron-astrocyte coupling model to improve the recognition ability and the prediction and control of seizures.

Acknowledgements

Project supported by the National Natural Science Foundation of China (Grant Nos. 12132012 and 11972275) and the National Science Foundation for Young Scientists of China (Grant No. 12102240).

References

[1] Ip Y K and Chew S F 2010 *Front. Physiol.* **1** 134
[2] Cagnon L and Braissant O 2007 *Brain Res. Rev.* **56** 183
[3] Marcaggi P, Jeanne M and Coles J A 2004 *Eur. J. Neurosci.* **19** 966
[4] Cooper A J 2011 *Neurochem. Int.* **59** 456
[5] Waniewski R A 1992 *J. Neurochem.* **58** 167
[6] Martinez H A, Bell K P and Norenberg M D 1977 *Science.* **195** 1356
[7] Norenberg M D and Martinez H A 1979 *Brain Res.* **161** 303
[8] Weil M H 1962 *Neurochemistry.* 321
[9] Van den Berg C J 1969 *Handbook of Neurochemistry.* **3** 355
[10] Thrane V R, Thrane A S, Wang F, *et al.* 2013 *Nature Med.* **19** 1643
[11] Kucheryavykh Y V, Kucheryavykh L Y, Nichols C G, *et al.* 2007 *Glia.* **55** 274
[12] Butt A M and Kalsi A 2006 *J. Cell Mol. Med.* **10** 33
[13] Heuser K, Eid T, Lauritzen F, *et al.* 2012 *J. Neuropathol Exp. Neurol.* **71** 814
[14] Tong X, Ao Y, Faas G C, *et al.* 2014 *Nature Neuroscience.* **17** 694
[15] Cressman J R, Ullah G, Ziburkus J, *et al.* 2009 *J. Comput. Neurosci.* **26** 159
[16] David Y, Cacheaux L P, Ivens S, *et al.* 2009 *J. Neurosci Off. J. Soc. Neurosci.* **29** 10588
[17] Wei Y N, Ullah G and Schiff S J 2014 *J. Neurosci Off. J. Soc. Neurosci.* **34** 11733
[18] Wei Y N, Ullah G, Ingram J, *et al.* 2014 *J. Neurophysiol.* **112** 213
[19] Kager H, Wadman W J and Somjen G G 2000 *J. Neurophysiol.* **84** 495
[20] Du M M, Li J J, Yuan Z X, *et al.* 2020 *Chin. Phys. B.* **29** 038701
[21] Østby I, Øyehaug L, Einevoll G T, *et al.* 2009 *PLoS Comput. Biol.* **5** e1000272
[22] Øyehaug L, Østby I, Lloyd C M, *et al.* 2012 *J. Comput. Neurosci.* **32** 147
[23] Witthoft A, Filosa J A and Karniadakis G E 2013 *Biophys J.* **105** 2046
[24] Sibille J, Dao D K, Holcman D, *et al.* 2015 *PLoS Comput. Biol.* **11** e1004137
[25] Du M M, Li J J, Liang C, *et al.* 2018 *Plos Comput. Biology.* **14** e1005877
[26] Basile A S 2002 *Neurochem. Internat.* **41** 115
[27] Traynelis S F and Dingledine R 1988 *J. Neurophysiol.* **59** 259
[28] Ingram J M, Zhang C, Xu J, *et al.* 2013 *J. Neurosci Methods.* **214** 45
[29] Ziburkus J, Cressman J R, Barreto E, *et al.* 2006 *J. Neurophysiol.* **95** 3948
[30] Sivilotti L and Nistri A 1991 *Prog. Neurobiology.* **36** 35
[31] Knowles W D, Schneiderman J H, Wheal H V, *et al.* 1984 *Cellular Molecul. Neurobiology.* **4** 207
[32] Newberry N R and Nicoll R A 1984 *J. Physiology.* **348** 239
[33] Iles J F and Jack J J 1983 *Brain.* **103** 555
[34] Cooper A J and Plum F 1987 *Physiological Rev.* **67** 440
[35] Raichle M E and Larson K B 1981 *Circ. Res.* **48** 913
[36] Dombro R S, Hutson D G and Norenberg M D 1993 *Mol. Chem. Neuropathol.* **19** 259
[37] Norenberg M D 1987 *Neurochem. Pathol.* **6** 13
[38] Subbalakshmi G Y and Murthy C R 1983 *Neurochem. Int.* **5** 593
[39] Plum F and Hindfelt B 1976 *Handbook of Clinical Neurology* **27** 349
[40] Crossley I R, Wardle E N and Williams R 1983 *Clin. Sci.* **64** 247
[41] Lux H D and Neher E 1970 *Exp. Brain Res.* **11** 431
[42] Takahashi K, Kameda H, Kataoka M, *et al.* 1993 *Neurosci. Lett.* **151** 51